Marine and Petroleum Geology 26 (2009) 1365–1378

Contents lists available at ScienceDirect

Marine and Petroleum Geology

journal homepage: www.elsevier.com/locate/marpetgeo

# Tracing of deeply-buried source rock: A case study of the WC9-2 petroleum pool in the Pearl River Mouth Basin, South China Sea

X.M. Xiao [a,*], N.X. Li [a], H.J. Gan [a], Y.B. Jin [a], H. Tian [a], B.J. Huang [a,b], Y.C. Tang [c]

[a] State Key Laboratory of Organic Geochemistry, Guangzhou Institute of Geochemistry, Chinese Academy of Sciences, Wushan, Guangzhou 510640, China
[b] CNOOC Ltd, Zhanjiang 524057, China
[c] Power, Environmental, and Energy Research Center, California Institute of Technology, CA 91722, USA

ARTICLE INFO

*Article history:*
Received 4 September 2008
Received in revised form
21 February 2009
Accepted 25 February 2009
Available online 6 March 2009

*Keywords:*
Deeply-buried source rock
Fluid inclusion
Kinetic modeling
2D basin modeling
Wenchang A sag
Pearl River Mouth Basin

ABSTRACT

The identification of a deeply-buried petroleum-source rock, owing to the difficulty in sample collection, has become a difficult task for establishing its relationship with discovered petroleum pools and evaluating its exploration potential in a petroleum-bearing basin. This paper proposes an approach to trace a deeply-buried source rock. The essential points include: determination of the petroleum-charging time of a reservoir, reconstruction of the petroleum generation history of its possible source rocks, establishment of the spatial connection between the source rocks and the reservoir over its geological history, identification of its effective source rock and the petroleum system from source to trap, and evaluation of petroleum potential from the deeply-buried source rock. A case study of the W9-2 petroleum pool in the Wenchang A sag of the Pearl River Mouth Basin, South China Sea was conducted using this approach. The W9-2 reservoir produces condensate oil and gas, sourced from deeply-buried source rocks. The reservoir consists of a few sets of sandstone in the Zhuhai Formation, and the possible source rocks include an early Oligocene Enping Formation mudstone and a late Eocene Wenchang Formation mudstone, with a current burial depth from 5000 to 9000 m. The fluid inclusion data from the reservoir rock indicate the oil and the gas charged the reservoir about 18–3.5 Ma and after 4.5 Ma, respectively. The kinetic modeling results show that the main stages of oil generation of the Wenchang mudstone and the Enping mudstone occurred during 28–20 Ma and 20–12 Ma, respectively, and that the $\delta^{13}C_1$ value of the gas generated from the Enping mudstone has a better match with that of the reservoir gas than the gas from the Wenchang mudstone. Results from a 2D basin modeling further indicate that the petroleum from the Enping mudstone migrated upward along the well-developed syn-sedimentary faults in the central area of the sag into the reservoir, but that the petroleum from the Wenchang mudstone migrated laterally first toward the marginal faults of the sag and then migrated upward along the faults into shallow strata. The present results suggest that the trap structure in the central area of the sag is a favorable place for the accumulation of the Enping mudstone-derived petroleum, and that the Wenchang mudstone-derived petroleum would have a contribution to the structures along the deep faults as well as in the uplifted area around the sag.



## 1. Introduction

Source rock identification is an important task in evaluating a petroleum-bearing basin since it is directly related to its petroleum resource potential and exploration directions. Organic geochemistry is commonly used for oil/gas-source correlation (Tissot and Welte, 1984; Magoon and Dow, 1994). This method is based on similarities mainly in chemical and isotopic compositions between the reservoir petroleum and the residual oil and gas from its possible source rocks to determine their original relation. For oil-source rock correlation, biomarkers such as normal alkane, sterane and terpane distribution and other parameters are effective and widely applied (Seifert and Moldowan, 1978; Peters and Moldowan, 1993; Zhang et al., 2001; Liang and Chen, 2005). Carbon and hydrogen isotope ratios of whole oil, extracts from source rocks, and their fractions have been useful to identify oil origin types and establish oil-source rock correlations (Stahl, 1978; Robinson and Himer, 1991; Sun et al., 2000; Liu et al., 2007). However, gas-source correlation is much more difficult since available information from gas is limited. Carbon and hydrogen isotope ratios of gas, coupled

* Corresponding author. Tel.: +86 20 8529 0176; fax: +86 20 8529 0706.
*E-mail address:* xmxiao@gig.ac.cn (X.M. Xiao).

0264-8172/$ – see front matter © 2009 Elsevier Ltd. All rights reserved.
doi:10.1016/j.marpetgeo.2009.02.009

with its composition parameters have been widely suggested for this purpose (Schoell, 1980; James, 1983; Littke et al., 1999). Rare gas isotopes (Liu et al., 2001), parameters of $C_{6-8}$ light hydrocarbons (Li et al., 2001; Liu et al., 2003a) and carbon isotopes of benzene and toluene (Jiang et al., 2000; Lao et al., 2002) are also believed to be helpful for source identification of gas.

It is obvious that the above methods and parameters are suitable only to petroleum-bearing basins where both petroleum and source rock samples are available. However, commercial oil and gas reservoirs are frequently derived from deeply-buried source rocks in some large-scale basins. For instance, the Cambrian–Ordovician source rock has a burial depth over 10,000 m in the Manjiaer Depression of the Tarim Basin, NW China (Xiao et al., 2000); the Tertiary source rock is overlain by sediment with thickness ranging from 7000 to 10,000 m in the central area of the Bozhong Depression in the Bohai Bay Basin, NE China (Hao et al., 2007); and some gas fields in the Yinggehai–Qingdongnan basins, South China Sea, are documented to be sourced from an Eocene mudstone with a current burial depth over 7000 m (Huang and Xiao, 2002; Huang et al., 2003). It is difficult to obtain source rock samples from these basins or depressions for making a direct oil/gas-source rock correlation, and the identification of their petroleum-source rock has become problematic in current petroleum exploration activities.

Fortunately, some methods and technologies, such as a refined fluid inclusion analysis of reservoir rocks (Mclimans, 1987; George et al., 1997; Xiao et al., 1996, 2002; Munz, 2001; Parnell et al., 2001; Liu et al., 2003b; Tao et al., 2003), petroleum generation kinetics, and gas carbon isotopic fractionation kinetic modeling of source rocks (Tissot et al., 1987; Ungger and Pelet, 1987; Pepper and Corvit, 1995; Tang et al., 2000; Xiao et al., 2005, 2006), and 2D and 3D basin modeling (Ungerer et al., 1990; Inan et al., 1997; Mann et al., 1997; Schneifer and Wolf, 2000; Lutz et al., 2004; Justwan et al., 2006; Lampe et al., 2006), can provide information related to petroleum origin in reservoirs and deeply-buried source rocks. The aim of this paper is to present an approach to tie a deeply-buried source rock to a petroleum reservoir using integrated geological and geochemical techniques through a case study of the W9-2 petroleum pool in the Wenchang A sag of the Pearl River Mouth Basin, South China Sea.

## 2. Approach

It is often difficult to make a direct connection of a deeply-buried source rock with a reservoir petroleum by the conventional geochemical parameters and methods due to lack of source rock samples. Our proposed approach to solve this problem is based on the following considerations: there should be a match between the formation time of the targeting trap structure, the petroleum-charging time of the reservoir and the petroleum generation history of its source rock; the reservoir should be connected to its source rock by some pathways to form a system over geological history; and the petroleum-source rock relationship established by this time and spatial constraint could be explainable by available geochemical data from the petroleum system. The framework of this approach is shown in Fig. 1. The key points are further described below.

(1) We investigated petroleum-charging time for a target petroleum pool first. The most common and effective approach is to use fluid inclusion analysis of reservoir rocks (Aplin et al., 1999, 2000; Parnell et al., 2001; Liu et al., 2003b). Although some geothermometer methods such as clay minerals (Liewig et al., 1987; Hamilton et al., 1989), Ar–Ar isotopes (Wang et al., 2005), and reservoir bitumen reflectance (Xiao et al., 2001; Wang et al., 2002) have been also applied for this purpose, they were not used in this study. By combining trapping temperatures and pressures of hydrocarbon inclusions or their coeval aqueous inclusions with the thermal history of their host rock (Aplin et al., 1999, 2000; Liu et al., 2003b), we can deduce the phases and times for the petroleum-charging of the reservoir.

(2) Using petroleum generation kinetic modeling establishes the petroleum generation history of the possible source rocks (two or three sets of mudstone in most cases) of the reservoir and in turn outlines their main stages of petroleum generation (Hosgormez and Yalcin, 2005). For a reservoir with natural gas present, methane carbon isotope kinetic modeling of the assumed source rocks is strongly suggested to establish the $\delta^{13}C_1$ fractionation geological models of their generated gases. A comparison between those models and the measured $\delta^{13}C_1$ value of the reservoir gas can usually help to select a probable source rock (Xiao et al., 2005, 2006). The crucial point of the kinetic modeling is to obtain immature or low-mature source rock samples which are representative of the deeply-buried source rocks in terms of geological age, sedimentary facies, and in particular kerogen types for pyrolysis experiments and kinetic parameter computation.

(3) 2D basin modeling is conducted to reconstruct the petroleum generation, migration and accumulation history of the possible source rocks and to examine the spatial connection of the reservoir to the source rocks over geological history (Inan et al., 1997; Mann et al., 1997; Lampe et al., 2006). This work makes a further correlation between the reservoir and the probable source rock suggested through the above analysis.

(4) The petroleum system is proposed according to the petroleum-source correlation from this investigation. Integrated with available geological and geochemical characteristics, the petroleum potential from the deeply-buried source rock is evaluated and the exploration directions are suggested for the petroleum system.

## 3. Identification of the source rock of the WC9-2 petroleum pool

### 3.1. Geological setting

The Wenchang A sag, located in the western part of the Pearl River Mouth Basin, South China Sea (Fig. 2), is the largest sub-depression of the Wenchang Depression, covering an area of 3350 $km^2$ (Feng and Liu, 1999; Ji and Wang, 2004). The Tertiary strata, deposited directly on the pre-Tertiary basement, reaches a thickness of 6000–9000 m in the central area of the sag, 4000–6000 m in the basin margin, and 3000–4000 m along the basin fringe. The stratigraphy includes the Wenchang Formation, Enping Formation, Zhuhai Formation, Zhujiang Formation, Hanjiang Formation, Yuehai Formation, Wanshan Formation and Qionghai Formation (Fig. 3). These strata comprise a source-reservoir-cap combination. The Wenchang and Enping formations contain thick dark mudstones as source rocks, the Zhuhai and Zhujiang formations contain sandstones as reservoirs, and the Hanjiang and Yuehai formations are regional cap rocks (Lin and Sun, 1999; Huang et al., 2007).

The W9-2 petroleum pool is located at the central area of the Wenchang A sag (Fig. 2). The trap is a fault-block structure. The reservoir is a few sets of sandstone in the Zhuhai Formation, and produces light oil and natural gas. The reservoir fluid is a typical condensate, characterized by a low density, low condensate point, low sulfur content, low wax content and low asphaltene content (Huang et al., 2003). The gas contains 90–94% hydrocarbon gas and

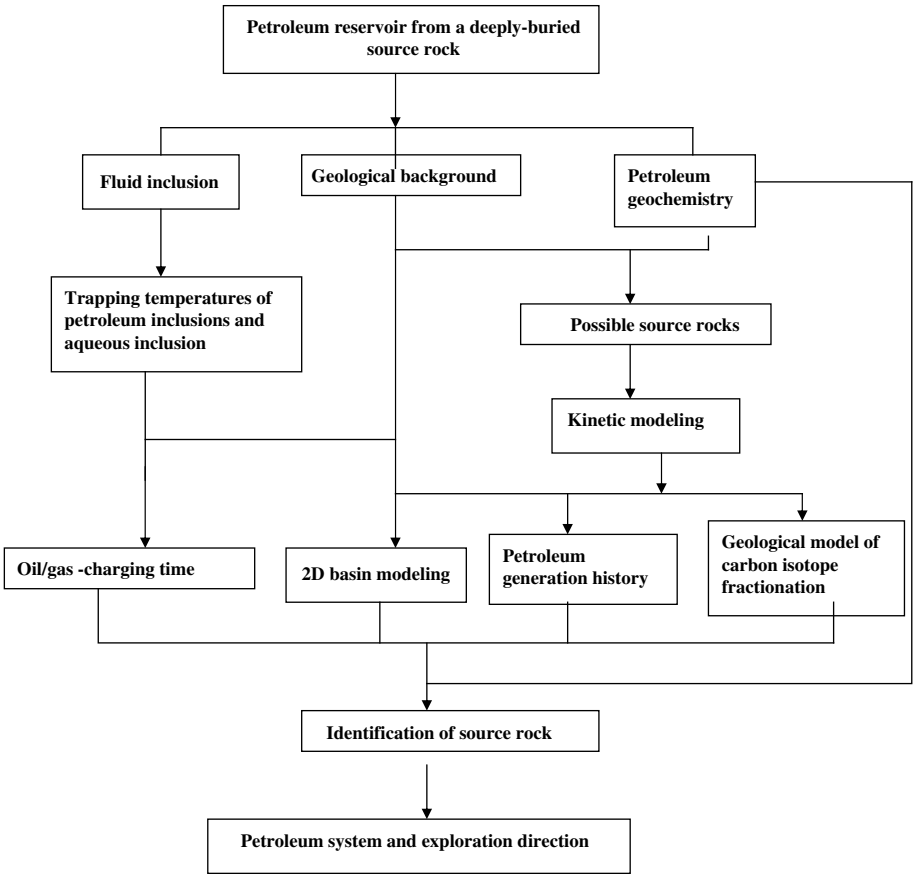


**Fig. 1.** Sketch map outlining the approach to trace deeply-buried source rocks. See details in text.

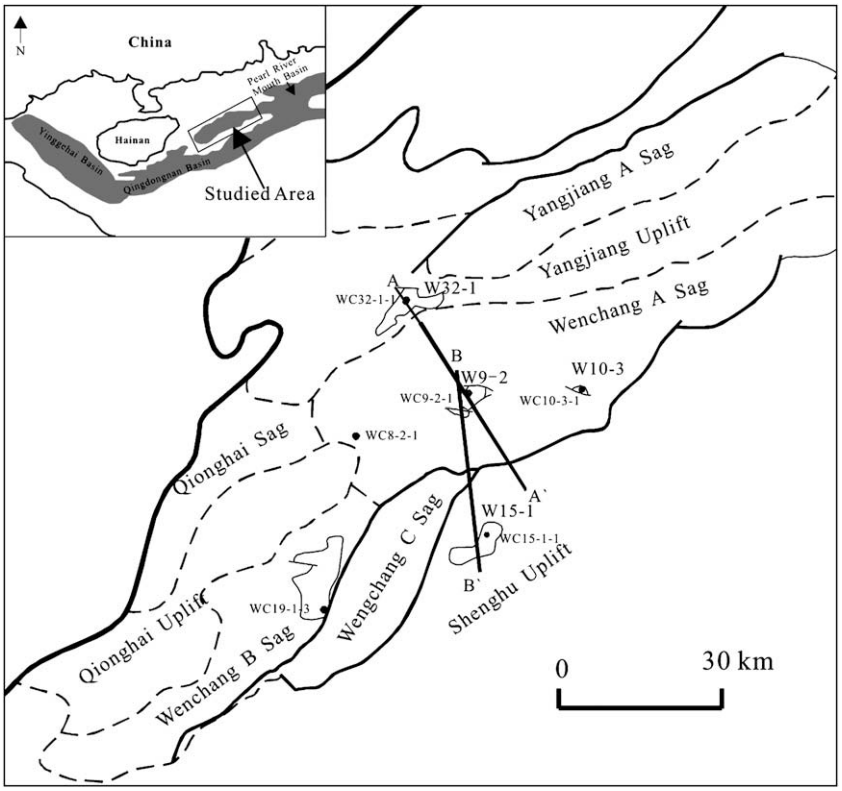


**Fig. 2.** Sketch map showing the location and structural setting of the Wenchang A sag (modified from data from CNOOC Limited, Zhanjiang).

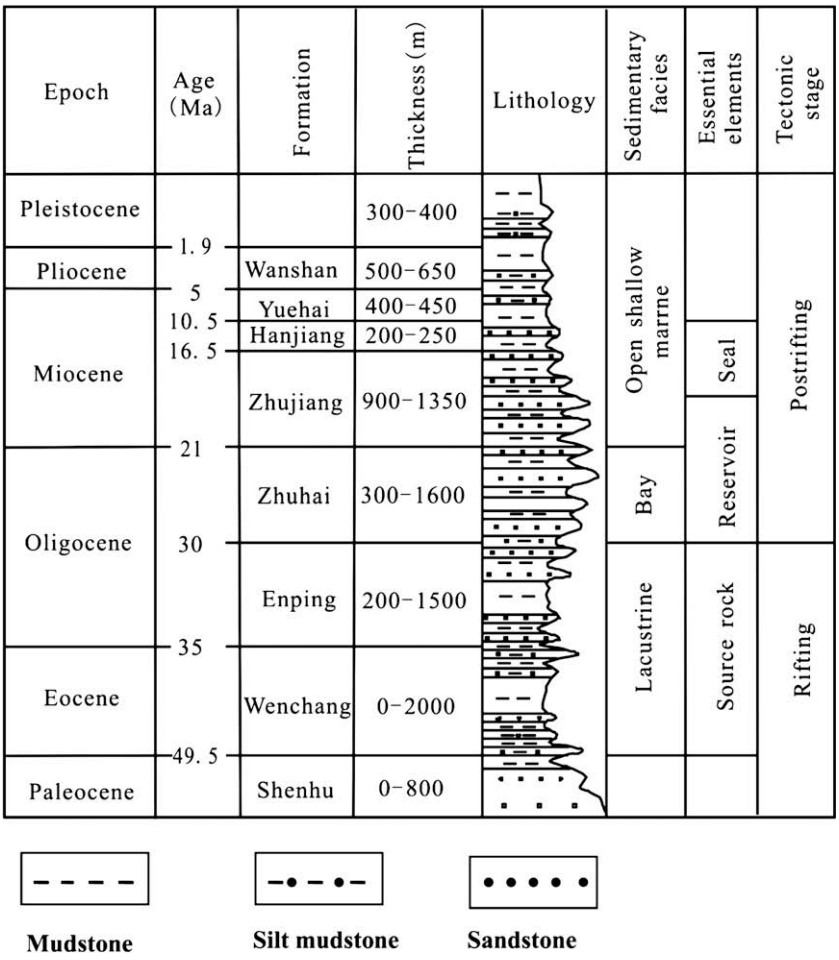


**Fig. 3.** Schematic stratigraphic column of the Wenchang A sag (modified from data from CNOOC Limited, Zhanjiang).

6–10% non-hydrocarbon gas, and the hydrocarbon gas is dominated by methane, with a dryness index of 0.79–0.88 (within the range of the wet gas, Table 1). The $\delta^{13}C$ values of $C_1$, $C_2$ and $C_3$ of the gas are −38.5 to −41.68‰, −28.30 to −30.66‰ and −25.56 to −27.23‰, respectively (Table 1).

Both the Wenchang and Enping formations contain significant amount of dark mudstone observed in borehole samples from the uplifted area of the sag and other Wenchang sub-depressions. The Wenchang mudstone has a TOC content of 0.27–4.57%, with an average of 1.73%, and has mainly a HI (hydrogen index from Rock–Eval analysis) of 300–600 mg/g TOC, indicating mainly a Type II kerogen (Huang et al., 2007). The Enping mudstone has a TOC content of 0.29–8.53%, with an average of 1.56%. The HI is mainly within 100–300 mg/g TOC (Ji and Wang, 2004; Huang et al., 2007), and the H/C (atomic ratio of hydrogen to carbon) and O/C (atomic ratio of oxygen to carbon) of the kerogen range mainly from 0.6 to 1.1 and 0.13 to 0.25, respectively (Liang, 1989), indicating mainly a Type III kerogen.

The Wenchang Formation and Enping Formation have a thickness of 1500–2000 m and 1000–1500 m, respectively, in the central area of the Wenchang A sag (Huang et al., 2007). Thick dark mudstone exists in both formations based on the available borehole data and seismic interpretation from this sag (Ji and Wang, 2004). Moreover, a few commercial petroleum pools such as the W9-2, W9-3 and W10-3 have been found in the central area of the sag (Fig. 2) and their petroleum was reported to be derived from the deeply-buried strata (i. e., the Wenchang and Enping formations) though vertical migration into the reservoir since there is no other source candidate on the basis of the geological background (Ji and Wang, 2004; Huang et al., 2007). Further work was needed to determine if the Wenchang Formation, the Enping Formation, or both are the main source rocks of the petroleum pools in the central area of the sag. Solving this problem will help guide the petroleum efforts for this sag. This paper uses the W9-2 petroleum pool as a case study to 1) trace its deeply-buried source rock using the

**Table 1**
Chemical compositions and carbon isotope ratios of reservoir gas from the well of WC9-2-1 (data from CNOOC Ltd.).

| Sample depth (m) | Formation | Composition (%) | | | | | Carbon isotope ratio $\delta^{13}C$ (‰) | | | |
|---|---|---|---|---|---|---|---|---|---|---|
| | | $N_2$ | $CO_2$ | $C_1$ | $C_2^+$ | $C_1/\sum Cn$ | $C_1$ | $C_2$ | $C_3$ | $CO_2$ |
| 3153.7 | Zhuhai 1 | 0.16 | 5.30 | 77.77 | 16.78 | 0.82 | −38.25 | −29.86 | −27.23 | −11.34 |
| 3661–3699 | | 1.10 | 6.16 | 76.39 | 14.67 | 0.84 | −39.69 | −29.57 | −26.62 | −7.88 |
| 3770–3799 | Zhuhai 2 | 1.36 | 5.24 | 72.84 | 18.82 | 0.79 | −41.69 | −29.98 | −27.47 | −8.22 |
| 3968–4000 | | 1.40 | 6.30 | 77.88 | 10.63 | 0.88 | −39.16 | −28.30 | −25.56 | −4.16 |

approach outlined above, 2) propose the relative petroleum system, and 3) discuss further exploration implications for the area.

### 3.2. Reservoir fluid inclusion analysis and petroleum-charging time

#### 3.2.1. Fluid inclusion investigation

A detailed fluid inclusion investigation was conducted for the Zhuhai Formation reservoir sandstones from depth ranging from 3204 to 3785 m from the wells of WC9-2-1 and WC9-2-2 in the W9-2 petroleum pool (Fig. 2). The sandstones contain abundant secondary fluid inclusions in fissures and enlarged overgrowths of quartz grains, including aqueous inclusions and organic inclusions, and $CO_2$ inclusions. Aqueous inclusions are the dominant type, usually showing dark yellow fluorescence on their inner edge from condensate oil (Fig. 4a and b). The organic inclusion has two types: hydrocarbon gas inclusion and petroleum inclusion. The hydrocarbon gas inclusion occurs widely, sometimes associated with the aqueous inclusion (Fig. 4e). The petroleum inclusion was only observed in a few samples, occurring in micro-fissures in quartz grains, with green-yellow fluorescence (Fig. 4c and d). $CO_2$ inclusions or the $CO_2$-bearing inclusions occur occasionally, and were also found in micro-fissures in quartz grains, associated with aqueous inclusions and hydrocarbon gas inclusions (Fig. 4f). Therefore, the fluid inclusion type and distribution is consistent with the current reservoir fluid composition (condensate oil, hydrocarbon gas and $CO_2$ gas).

The homogenization temperature of a fluid inclusion is related to its trapping temperature although it is not identical in most cases (Aplin et al., 2000; Liu et al., 2003b). The present study focused on the homogenization temperatures of both the petroleum inclusion and the aqueous inclusion coeval with the hydrocarbon gas inclusion since they are directly related to petroleum-charging conditions and history. The homogenization temperatures of the petroleum inclusion have a wide range, from 82 to 127 °C, with an average of about 110 °C, and the homogenization temperatures of the aqueous inclusion have a smaller range, from 123 to152 °C, with an average of about 140 °C (Fig. 5).

#### 3.2.2. Petroleum-charging time

The homogenization temperature of a petroleum inclusion is usually considered as its minimum trapping temperature, and cannot represent its trapping temperature in normal cases according to its P–T phase diagram (Aplin et al., 1999). Some approaches have been developed to obtain the trapping temperature of a petroleum inclusion from its homogenization temperature through a PVT analog computation (Aplin et al., 2000; Liu et al., 2003b). However, these approaches are not suitable for the case of the W9-2 petroleum pool since we have not found a situation where both petroleum inclusion and its coeval aqueous inclusion occur in the same fissure or mineral grain of the studied samples. In this case, a simple alternative method to deduce the trapping temperature of a petroleum inclusion from its homogenization

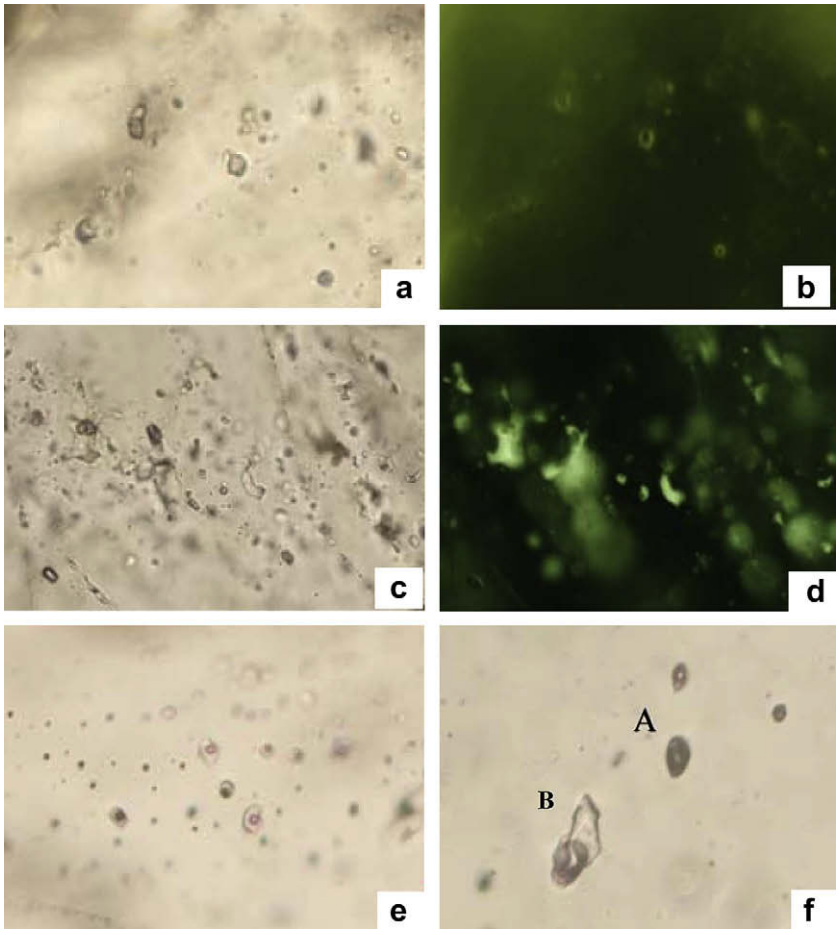


**Fig. 4.** Photomicrographs showing different types of fluid inclusions from the W9-2 reservoir rocks. (a) Aqueous inclusions, Zhuhai Formation sandstone, WC19-1-1, transmitted light, 450×. (b) Aqueous inclusions outlined by light yellow fluorescence from condensate oil, the same field with (a), fluorescent mode, 450×. (c). Petroleum inclusions, Zhuhai Formation sandstone, WC19-2-1, transmitted light, 450×. (d) The same field with (c), fluorescent mode, 450×. (e) Coeval gaseous and aqueous inclusions, Zhuhai Formation sandstone, WC19-2-2, transmitted light, 450×. (f) Coeval hydrocarbon gas inclusions (A) and $CO_2$-bearing inclusions (B), Zhuhai Formation sandstone, WC19-2-2, transmitted light, 450×.

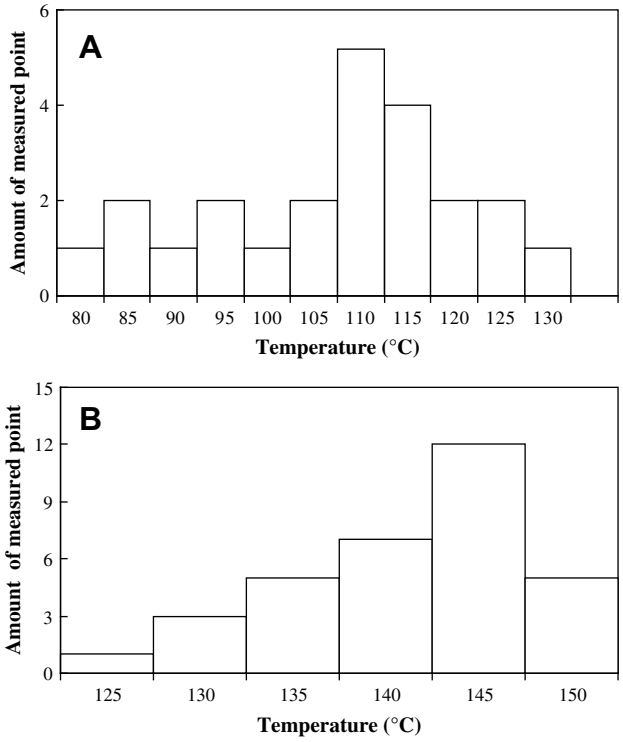


**Fig. 5.** Histograms showing homogenization temperature distribution of petroleum inclusions (A) and aqueous inclusions coeval with gas inclusions (B) in the Zhuhai Formation reservoir sandstone from the wells of WC9-2-1 and WC9-2-2. The burial depth of the samples ranges from 3204 to 3785 m.

temperature is usually suggested. For instance, both Aplin et al. (2000) and Swarbricka et al. (2000) used the homogenization temperature of aqueous inclusions to represent the trapping temperature of petroleum inclusions to investigate the PVTX history of the North Sea's Judy oilfield. In their cases, the homogenization temperature of the aqueous inclusions is 15–20 °C greater than that of the petroleum inclusions. However, according to the results from Liu et al. (2003b), Mi et al. (2004) and Wang et al. (2006), for a reservoir with higher mature oil or hydrocarbon gas, the difference between the trapping and homogenization temperature of its petroleum inclusion is within the range of 5–10 °C. Because the W9-2 reservoir is filled with condensate oil and hydrocarbon gas, we used 5–10 °C as the difference between the trapping and homogenization temperature of its petroleum inclusions.

Since no useful temperature data can be obtained from the hydrocarbon gas inclusions, their coeval aqueous inclusions were selected for the measurement of homogenization temperature. The only way in which the homogenization temperature of an aqueous inclusion can represent its trapping temperature is that the aqueous inclusion is saturated by gas (Liu and Shen, 1999). Fluids in the studied reservoirs contain natural gases and the aqueous inclusion is considered to be saturated by gas, so that it is assumed that its homogenization temperature can approximately represent its trapping temperature.

The trapping time of the petroleum inclusions and gas inclusions can be inferred from their trapping temperatures deduced by the above method, coupled with the thermal history of their host rocks. In Fig. 6, the thermal history of the studied samples was obtained according to the strata data from CNOOC Limited, Zhanjiang, and a paleo-geothermal gradient of 3.6 °C/100 m from ECPGC (1992). The sample from the well of WC9-2-1 has a depth of 3668.5 m. Its petroleum inclusions have the homogenization temperatures of 82–116 °C, with an average of 105 °C. The corresponding trapping temperature would range from 87–92 °C to 121–126 °C. Therefore, the petroleum inclusions from the sample were trapped from 18–17.5 Ma to 4.5–3.5 Ma (Fig. 6A). The sample with a depth of 3765.4–3768.2 m from the well of WC9-2-2 contains a lot of gas inclusions. The aqueous inclusions coeval with the gas inclusions have the homogenization temperature of 126–150 °C, with a main population of 145 °C. The inclusions were trapped from 4.5 Ma, and up to the present time (Fig. 6B).

According to above discussion, the W9-2 reservoir has been charged by oil during middle and late Miocene, and by gas from Pliocene to the present, and it is still in the main stage of gas charging.

### 3.3. Kinetic modeling of possible source rocks

#### 3.3.1. Method and parameters

The possible source rocks of the W9-2 petroleum pool are dark mudstones in the Wenchang–Enping formations in the central area of the Wenchang A sag. Although no borehole has reached the strata in this area to obtain mudstone samples for a direct petroleum-source rock correlation, the petroleum generation and methane carbon isotope fractionation geological models of the mudstones under the specific geological conditions of this area were achieved using kinetic modeling (Tang et al., 2000; Xiao et al., 2005, 2006). These models can help us to outline the petroleum generation history of the possible source rocks and to provide a comparison of $\delta^{13}C_1$ values between the modeled gas and the

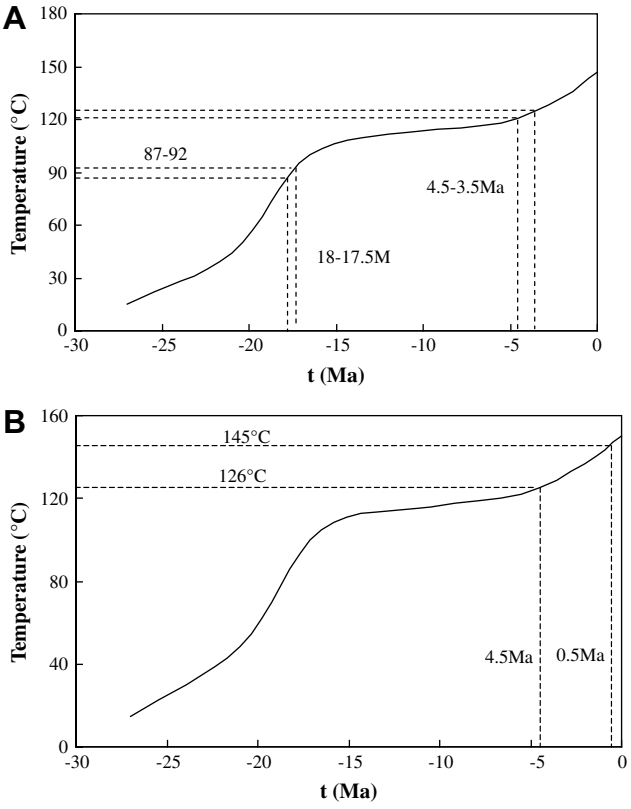


**Fig. 6.** Plots showing the formation time of petroleum inclusions for the well of WC9-2-1 (the sample depth is 3668.5 m) (A), and the formation time of aqueous inclusions coeval with gas inclusions for the well of WC9-2-2 (the sample depth ranges from 3768.2 to 3765.4 m) (B), by combining their deduced trapping temperatures with the inferred geothermal history of the host rocks. The strata data are from CNOOC Limited, Zhanjiang, and the paleo-geothermal gradient is 3.6 °C/100 m based on ECPGC (1992).

reservoir gas to trace the gas source. This method was applied by Xiao et al. (2005, 2006), and is summarized briefly here.

(1) Faults in the central area of the Wenchang A sag acted as vertical pathways for fluid migration. The petroleum in the W9-2 reservoir must come from source rocks buried deeply below. Faults and sandstone bodies compose the main pathway for upward petroleum migration in the Wenchang A sag (Ji and Wang, 2004). The possible source area should be in the area between points A and B where the total Tertiary sediment has a thickness from 7000 to 9000 m (Fig. 7). The Wenchang and Enping mudstones from the two points were selected for the kinetic modeling.

(2) The kinetic parameters used in the modeling are from a Wenchang mudstone sampled from the well of WC19-1-3 and an Enping mudstone from the well of WC8-2-1 (Fig. 2). The two samples are thermally immature, with Ro of 0.45% and 0.59%, respectively. Their hydrocarbon indexes (HI) are 444 mg/g TOC and 245 mg/g TOC, indicating Type II and Type III kerogens, respectively (Table 2). Although the well WC19-1-3 is located at another sag of the Wenchang Depression, these samples are considered representative of the whole Pearl River Mouth Basin according to the data of Huang et al. (2003).

(3) The kinetic parameters for petroleum generation and methane carbon isotopic fractionation of the two samples were reported by Gan (2006) and are presented in Tables 3 and 4, respectively. The experiment and method were described by Tang et al. (2000) and Xiao et al. (2005), but are summarized briefly here. Pyrolysis experiments on the two samples were conducted in gold tube reactors under anhydrous conditions. The samples were heated to the required temperatures ranging from 250 to 600 °C at rates of 2 °C/h and 20 °C/h, respectively. The kinetic parameters of petroleum generation and methane carbon isotopic fractionation were calculated and fitted using the software Kinetics 2000 and GOR-Isotope (GeolsoChem Corporation, 2003), respectively. This model uses a fixed frequency factor and a discredited Weibull-type activation energy distribution to calculate the kinetic parameters of the petroleum generation, and a uniform initial isotopic composition with variable activation energy offset (ΔEa) to calculate the kinetic parameters of methane carbon isotopic fractionation. The experimental data and calculated results based on the kinetic parameters for both hydrocarbon generation ($C_6+$, $C_{1-5}$ and $C_1$) and methane carbon isotopic fractionation of the two samples are presented in Figs. 8 and 9, respectively.

(4) The current geothermal gradient of the well of WC9-2-1 is 3.6 °C/100 m and the sea bottom temperature of the Wenchang A sag is 15 °C(ECPGC, 1992). They are respectively used as the paleo-geothermal gradient and the average paleo-surface temperature during the Tertiary (ECPGC, 1992; Gong, 2004). The middle of each of the Wenchang Formation and the Enping Formation beneath the points A and B was selected for this modeling (Fig. 7).

(5) The software used for geological extrapolation of the kinetic parameters in the present study is the GOR-Isotope (1.48) developed by GeolsoChem Corporation (2003). Its extensive functions include the modeling of the petroleum generation history as well as the modeling of methane carbon isotope fractionation for a selected source rock sample by combining the kinetic parameters with geothermal history of the sample (Tang et al., 2000). Successful applications to China petroleum-bearing basins have been widely reported, such as Gao et al. (2004), Xiao et al. (2005, 2006) and Tian et al. (2007).

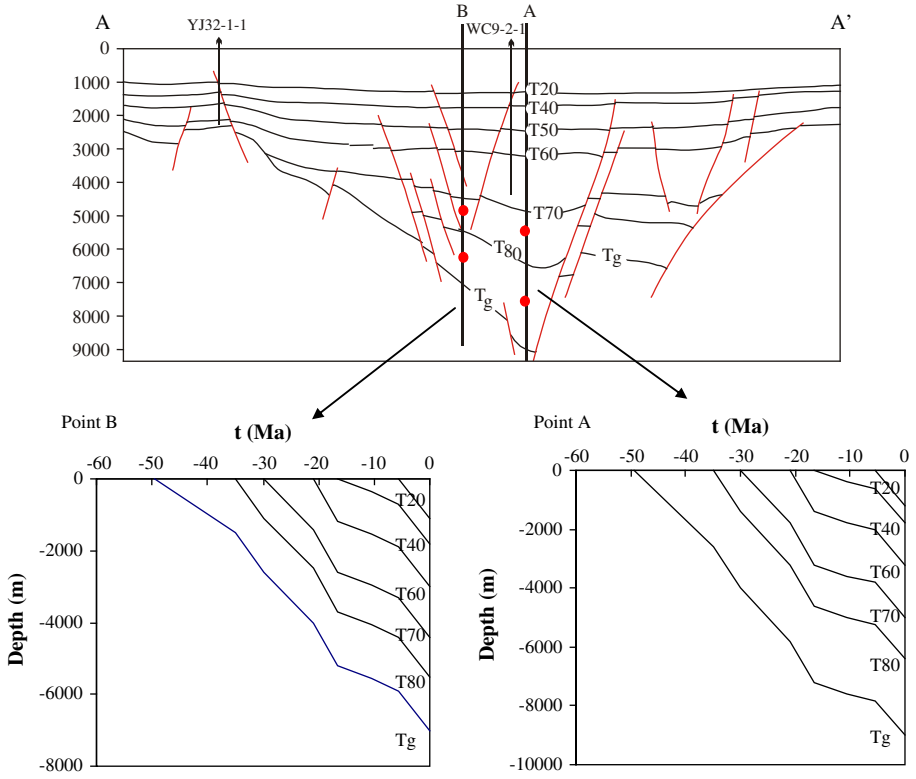


**Fig. 7.** Profile based on a seismic section through the Wenchang A sag. The buried history of the strata from points A and B selected for the kinetic modeling is presented. Data are from CNOOC Limited, Zhanjiang.

**Table 2**
Geological and geochemical characteristics of selected dark mudstones for thermal pyrolysis experiments from the Wenchang Depression.

| Well | Depth (m) | Formation | Sample | TOC (%) | VRo (%) | Rock–Eval analysis | | | |
|---|---|---|---|---|---|---|---|---|---|
| | | | | | | $S_1$ (mg/g) | $S_2$ (mg/g) | Tmax (°C) | HI (mg/g TOC) |
| WC19-1-3 | 1973–1982 | Wenchang | Kerogen from dark mudstone | 53.59 | 0.451 | 13.88 | 237.68 | 432 | 444 |
| WC8-2-1 | 2625 | Enping | | 55.46 | 0.592 | 34.71 | 135.66 | 443 | 245 |

*3.3.2. Petroleum generation history of possible source rocks*

Figs. 10 and 11 show the modeled results of the petroleum generation history and methane carbon isotope fractionation geological model of the Wenchang mudstone and the Enping mudstone from the selected points. For the Wenchang mudstone, the oil window occurred during 30–18 Ma, with the main stage of oil generation during 28–20 Ma. Its gas generation occurred from 23 to 7 Ma, with the main stage of gas generation between 21 and 2 Ma. The gas generated from the Wenchang mudstone has a cumulative $\delta^{13}C_1$ value of −34.0 to −39.8‰, and an instantaneous $\delta^{13}C_1$ value of −13.0 to −26‰ (Fig. 10). For the Enping mudstone, the oil widow spans a wide range from 21 to 7 Ma, with the main stage of oil generation during 20–12 Ma. Its gas generation started from 14 Ma and main stage of gas generation started from 10 Ma, with a current $C_{1-5}$ fraction conversion of 0.72 (Point A)–0.39 (Point B). Its generated gas has a cumulative $\delta^{13}C_1$ value of −38.5 to −44‰, and an instantaneous $\delta^{13}C_1$ value of −31 to −39‰ (Fig. 11).

*3.3.3. Identification of petroleum-source rock*

In a complete petroleum system, the main stages of oil generation from the effective source rock should be later than the formation time of the trap. The W9-2 trap began to develop during the middle Miocene, and its regional cap rock formed during late Miocene time (Ji and Wang, 2004). Therefore, its effective petroleum accumulation should occur during post-late Miocene time, i.e., after 16.5 Ma. Table 5 presents a comparison between the oil generation history of the possible source rocks and the petroleum-charging time of the reservoir for the W9-2 light oil. The main stage of oil generation of the Wenchang mudstone occurred during 28–20 Ma. This is obviously earlier than the trapping time (18–3.5 Ma) of the petroleum inclusions in the reservoir rock as well as earlier than the formation time of the trap. Therefore, the Wenchang mudstone is not the effective source rock of the light oil. The oil window and the main stage of oil generation of the Enping mudstone span a time range appropriate for both the trapping time of the petroleum inclusions and the formation time of the trap. Oil generated from the Enping mudstone could accumulate in the reservoir if migration pathways existed (see next section).

The gas generation periods of the Wenchang mudstone and the Enping mudstone exhibit considerable overlap (Table 6), which leads to an uncertainty when deducing the source rock of the W9-2 reservoir gas only from the trapping time of the aqueous inclusion. A comparison between the $\delta^{13}C_1$ value of the reservoir gas and the $\delta^{13}C_1$ value of the modeled gases from the selected mudstones provides useful information regarding the identification of the source rock. As an effective gas-source rock, its gas generation period should overlap the gas-charging period of the reservoir. After the trap formation, the source rock still generated a significant amount of gas, with an obvious increase of the $C_1$ or $C_{1-5}$ fraction. Moreover, the gas generated from the source rock should match with the reservoir gas in compositions and carbon isotopic values. From the results presented in Table 6, both the Wenchang and Enping mudstones generated a lot of gas after the trap formation with a significant increment of the $C_{1-5}$ fraction conversion, and are still in their main stage of gas generation. However, the Wenchang mudstone generated gas has a much heavier $\delta^{13}C_1$ value (−24.1 to −34.2‰) than the reservoir gas (−38.25 to −41.69‰), and the Enping mudstone generated gas has a $\delta^{13}C_1$ value of −38.5 to −43.9‰, within similar range to the reservoir gas. The Enping mudstone should, therefore, be the main gas-source rock of the W9-2 petroleum pool, and the contribution from the Wenchang mudstone generated gas seems of less importance.

In a summary, both the oil and gas of the W9-2 reservoir are mainly derived from the Enping mudstone in the central area of the Wenchang A sag, with a current burial depth 6500–4500 m. This observation agrees with a previous geochemical investigation by Huang et al. (2003). They have noted that the light oil from the W9-2 petroleum pool is characterized by a high Pr/Ph value (2.61–2.65), a light $\delta^{13}C$ value (−29.51 to −29.54‰), little or no 4-methylsterane ($C_{30}$ 4-methylsteranes/$C_{29}$ regular steranes <0.1), and a relatively high amount of the bicadinanes (bicadinanes/$C_{30}$ hopane = 2.0–6.5), which are quite similar to the biomarkers of the Enping mudstone and totally different from the biomarkers of the Wenchang mudstone sampled from the Wenchang B sag. Although there is no dark mudstone sampled from the central area of the Wenchang A sag, it has been widely believed that the two sets of mudstones from the Wenchang B sag can be well compared with the two sets of mudstones from the Wenchang A sag in both kerogen types and source matter precursor according to the available geochemical data of the immature source rock samples from some boreholes along the sag fringe and the seismic stratigraphic interpretations from the two sub-sags (Ji and Wang, 2004; Zhang et al., 2003, 2004; Huang et al., 2007). Thus, it can be also inferred that the light oil of the W9-2 petroleum pool is mainly from the Enping mudstone from its organic geochemical characteristics.

### 3.4. Basin modeling

In order to further confirm the above petroleum-source rock correlation of the W9-2 petroleum pool which mainly based on

**Table 3**
Kinetic parameters of oil and gas generation of the selected kerogen samples from the Wenchang Depression (from Gan, 2006).

| Sample | Kinetics parameter | $C_1$ | $C_{1-5}$ | $C_6$+ | |
|---|---|---|---|---|---|
| | | | | Generation | Cracking |
| WC19-1-3 | Frequency factor (A) $s^{-1}$ | 1E+13 | 1.5E+13 | 3.5E+14 | 9.0E+13 |
| | Average activation energy (kcal/mol) | 61 | 59 | 53 | 58 |
| | Mean square deviation (%E) | 7 | 7 | 5 | 5 |
| WC8-2-1 | Frequency factor (A) $s^{-1}$ | 1E+13 | 1.2E+13 | 3.0E+14 | 8.0E+13 |
| | Average activation energy (kcal/mol) | 60 | 58.5 | 53 | 59 |
| | Mean square deviation (%E) | 7 | 7 | 4 | 4 |

**Table 4**
Methane isotope fractionation kinetic parameters of the studied kerogen samples from the Wenchang Depression (from Gan, 2006).

| Sample | Methane carbon isotope fractionation kinetic parameters[a] | | | | | |
|---|---|---|---|---|---|---|
| | $\alpha$ | $\beta_L$ (cal/mol) | $\beta_H$ (cal/mol) | $\mu$ (kcal/mol) | $\sigma$ (kcal/mol) | $\delta_{init}$ (PDB) |
| WC19-1-3 | 1.01 | 3.5 | 52.10 | 54,000 | 6.5 | −28.03 |
| WC8-2-1 | 1.01 | 3.5 | 54.16 | 54,000 | 6.5 | −29.99 |

[a] $\alpha$ = the ratio value of $^{13}A/^{12}A$; $\beta_L$ = the lowest activation energy difference; $\beta_H$ = the highest activation energy difference; $\mu$ = the mean activation energy of Sigmoid function; $\sigma$ = the variance of Sigmoid function; $\delta_{init}$ = the initial carbon isotope of methane precursor (Tang et al., 2000).

the consistency between the petroleum generation history of the Enping mudstone and the petroleum-charging time of the reservoir, a 2D basin modeling was conducted to establish their spatial connection over geological history. A cross-section from the well of WC9-2-2 to the well of WC15-1-1 was selected to model the fluid flow using the software of IES *PetroFlow*. In this modeling, the sedimentary sequences, lithologies and structural framework were based on the available seismic interpretations and well data based on the CNOOC Ltd. The paleo-geothermal gradient is 3.6 °C/100 m from ECPGC (1992). It was assumed, from the above discussion, that both the Wenchang and Enping formations contain significant amounts of dark mudstone in the central area of the sag. The Wenchang mudstone has an average TOC of 1.76% and a Type II kerogen, and the Enping mudstone has an average TOC of 1.56% and a Type III kerogen (see Section 3.1).

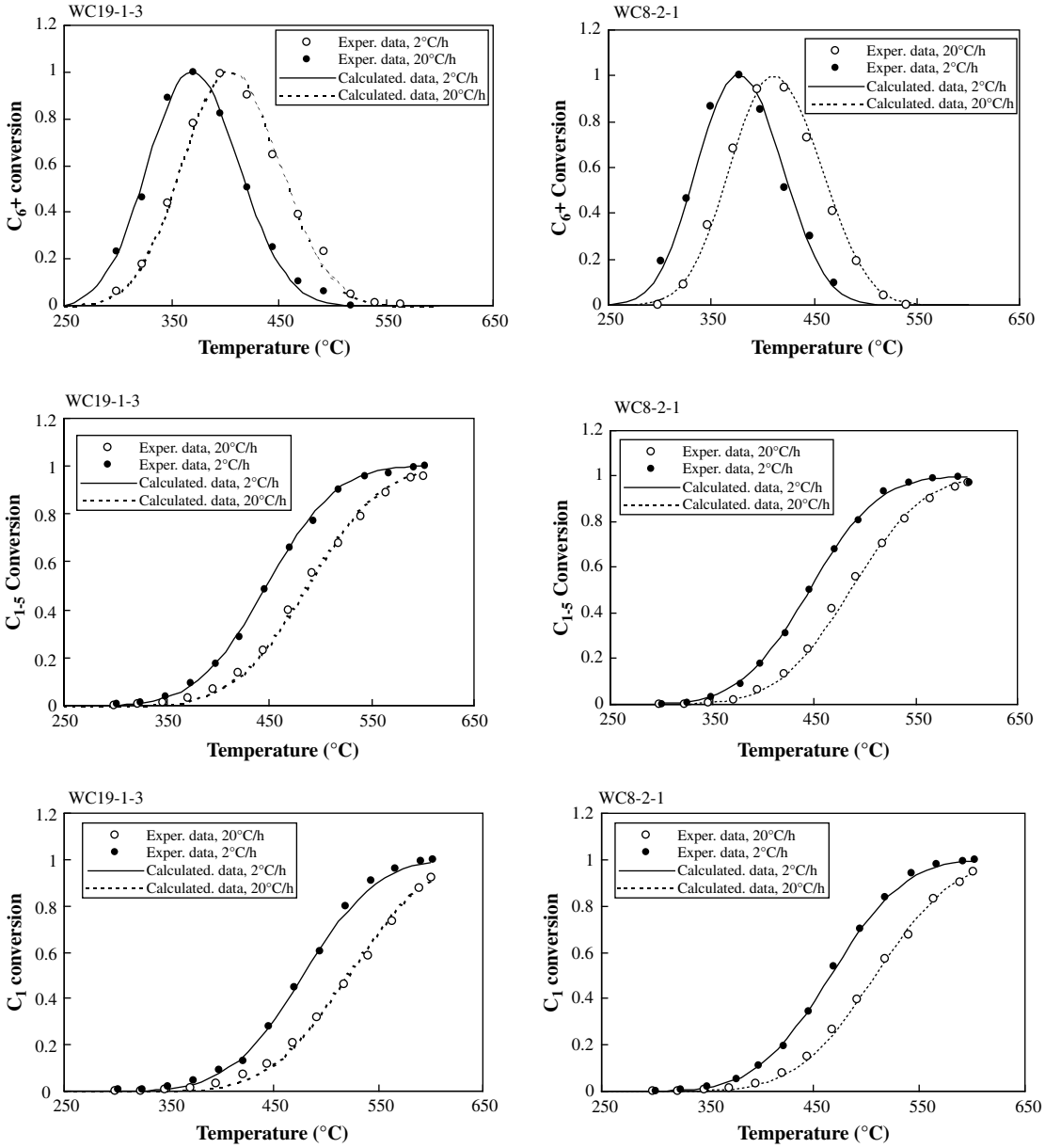


**Fig. 8.** A comparison of calculated oil ($C_{6+}$) and gas ($C_{1-5}$) generation conversion using the kinetic parameters from Table 3 with experimental data for the two studied kerogen samples. See details in text.

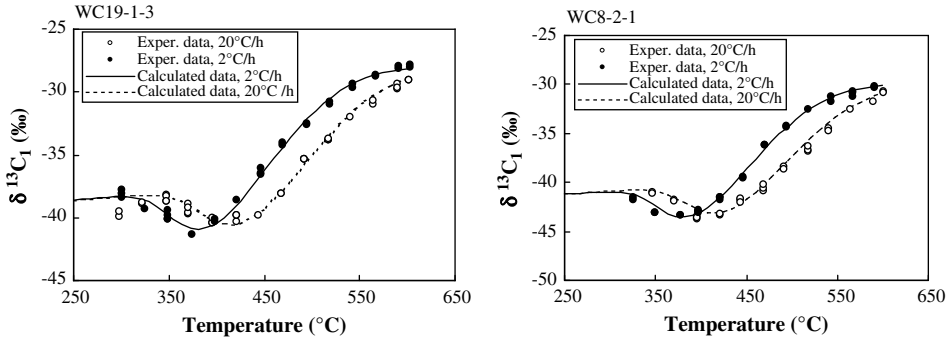


**Fig. 9.** The fitting of carbon isotopic fractionation of methane generated by sealed gold tube pyrolysis of the studied kerogen samples. The fitted kinetic parameters are presented in Table 4. See details in text.

The modeling result (Fig. 12) provides a general indication of the major petroleum-bearing flow directions in the section. The fluids migrate predominantly along faults, sandstone-rich strata and stratigraphic surfaces. The Enping Formation is overlain directly by the Zhuhai Formation and connected to the W9-2 reservoir rock by a series of syn-sedimentary faults. The petroleum migrated into the reservoir although a portion of early-generated petroleum might have dissipated because the trapping structure was not well developed. However, since the thick Enping Formation overlaying on the Wenchang Formation may have acted as a sealing rock in the

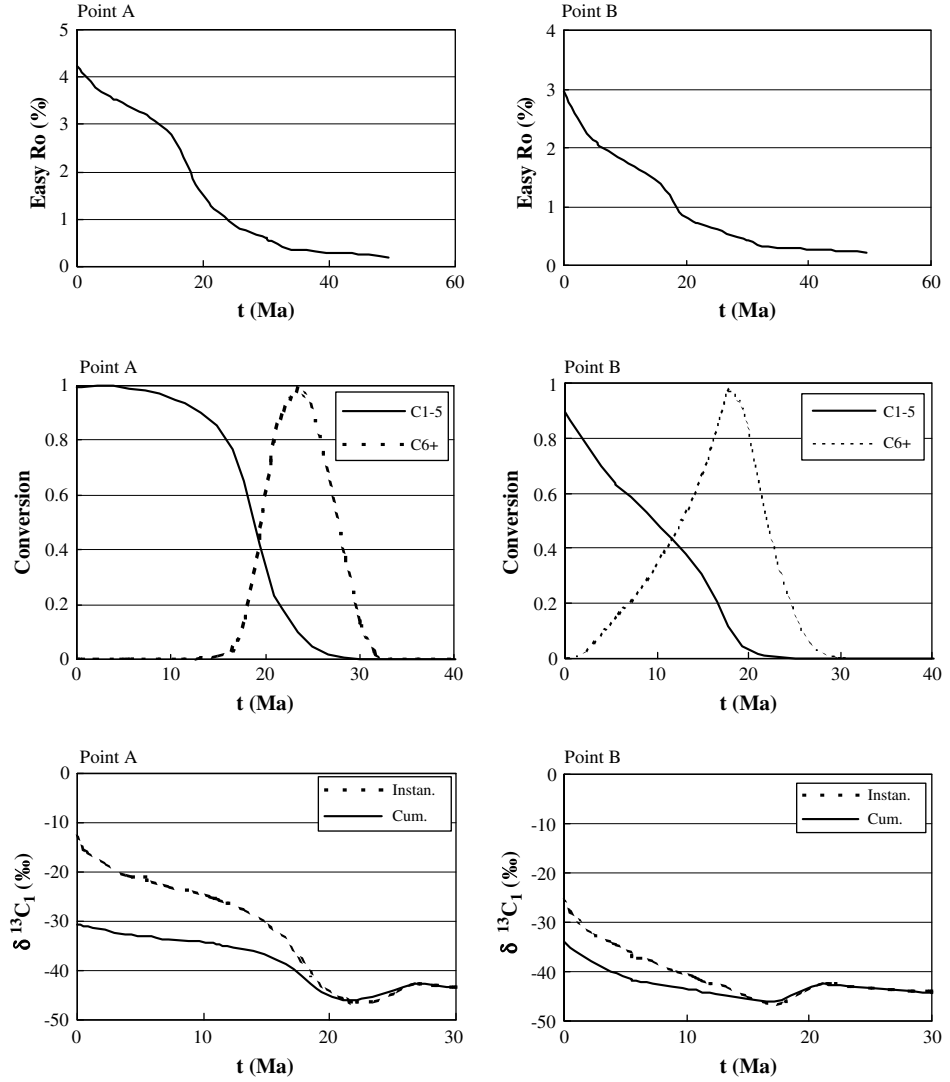


**Fig. 10.** Oil and gas generation and methane carbon isotopic fractionation kinetic models of dark mudstone in the Wenchang Formation from the two selected points. See details in text.

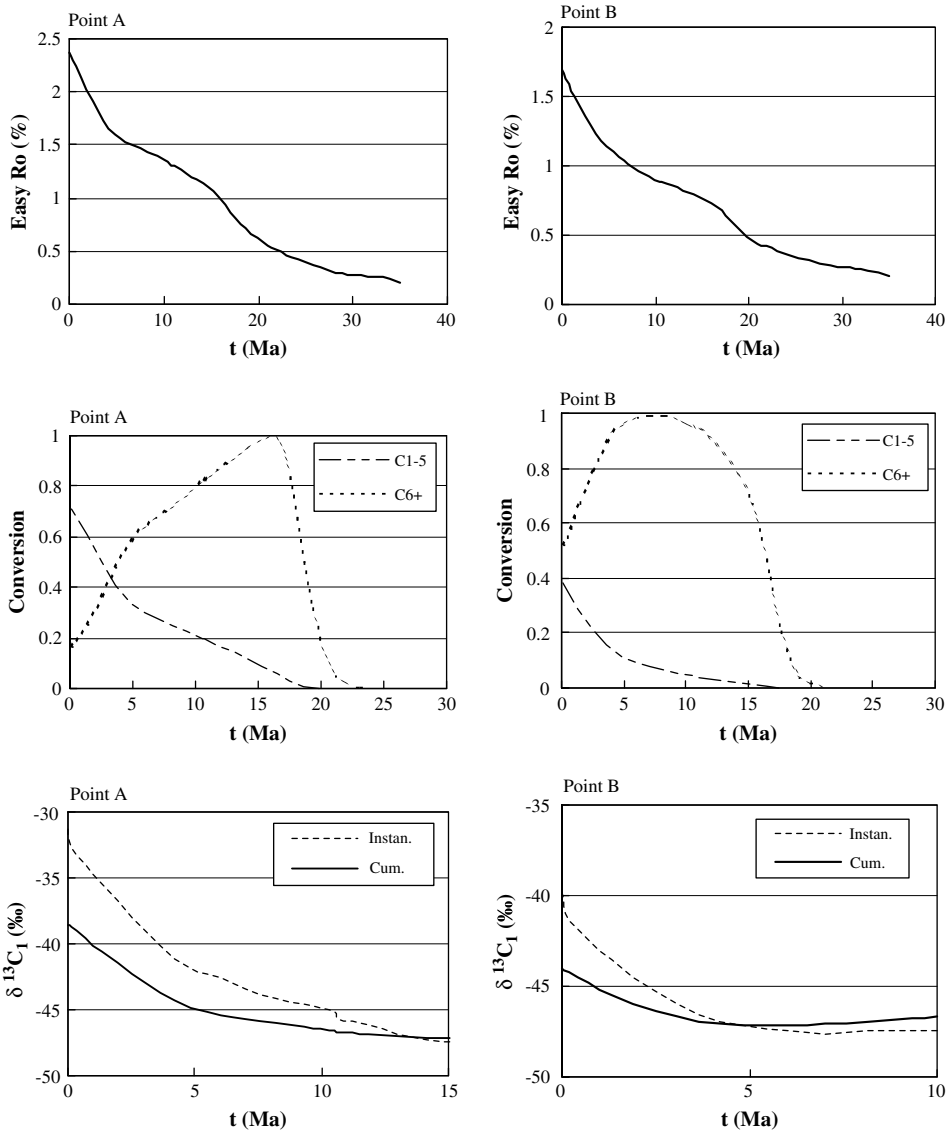


**Fig. 11.** Oil and gas generation and methane carbon isotopic fractionation kinetic models of dark mudstone in the Enping Formation from the two selected points. See details in text.

**Table 5**
Oil-source rock identification of the W9-2 petroleum pool.

| Oil-charging time based on petroleum inclusion data (Ma) | Timing of oil window of source rocks from the kinetic modeling | | | |
|---|---|---|---|---|
| | Point and source rock | Threshed of oil generation (Ma) | Main stages of oil generation (Ma) | Death line of oil generation (Ma) |
| 18–3.5 | Point A, Wenchang Formation | 30 | 28–24 | 23 |
| | Point B, Wenchang Formation | 26 | 25–20 | 18 |
| | Point A, Enping Formation | 21 | 20–17 | 15 |
| | Point B, Enping Formation | 18 | 17–12 | 7 |

central area of the sag, the petroleum from the Wenchang mudstone in this area had to migrate laterally toward the marginal faults, and then move upward along the faults into nearby overlying strata. The petroleum might have been trapped or dissipated in the overlying strata, or migrated along a combined pathway including faults and sandstone-rich strata to reach the structures in the uplifted area of the sag to form petroleum pools.

### 3.5. Petroleum system and exploration potential

We propose a petroleum system in the central area of the Wenchang B sag. For this petroleum system, the Enping mudstone is the main source rock, the Zhuhai–Zhujiang formations are reservoir and the Hanjiang–Yuehai formations are seal rock. Since the source rock mainly contains a Type III kerogen with a wide range of maturation levels, the W9-2 reservoir produces condensate oil and gas. The critical moment of the petroleum system was late Miocene when the source rock matured into the main stages of oil generation (Fig. 13). The generated petroleum from the Enping

**Table 6**
Gas-source rock identification of the W9-2 petroleum pool.

| Gas-charging time (Ma) | $\delta^{13}C_1$ value of reservoir gas (‰) | Timing of gas generation of source rocks from the kinetic modeling | | | | | | |
|---|---|---|---|---|---|---|---|---|
| | | Location and source rock | $C_{1-5}$ conversion | Gas threshed (Ma) | Main stage (Ma) | $\delta^{13}C_1$ value of cumulative gas (‰) | $\delta^{13}C_1$ value of instantaneous gas (‰) | $\delta^{13}C_1$ value of partly cumulative gas from 16.5 Ma (‰) |
| From 4.5 Ma to present day | 38.25–41.69 | Point A, Wenchang Formation | 1.00 | 23 | 21–15 | −29.8 | −13.1 | −24.1 |
| | | Point B, Wenchang Formation | 0.90 | 17 | 16–2 | −34.2 | −26.2 | −34.2 |
| | | Point A, Enping Formation | 0.72 | 14 | 10–0 | −38.5 | −31.3 | −38.5 |
| | | Point B, Enping Formation | 0.39 | 5 | 3–0 | −43.9 | −39.8 | −43.9 |

source rock migrated upward along the syn-sedimentary faults into the reservoirs to form the W9-2 petroleum pool.

There are two possible reasons why the petroleum from the Wenchang mudstone has not significantly contributed to the W9-2 reservoir: its oil generation was earlier than the formation time of the trap, and the thick Enping Formation acted as a sealing rock to prevent the petroleum from the Wenchang mudstone to migrate upward into the reservoir. Based on the 2D basin modeling, petroleum generated from the Wenchang mudstone would be prospective in earlier-formed trapping structures as well as the structures in the uplifted area around the sag. The discovery of the W10-3 petroleum pool (Fig. 2), close to the Zhu III deep fault (a marginal fault of the depression), produces oil with a density of 0.77–0.78 g/cm$^3$ from the lower section of reservoir sandstone of the Zhuhai Formation. The oil is characterized by a moderate concentration of $C_{30}$ 4-methylsteranes ($C_{30}$ 4-methylsteranes/$C_{29}$ regular steranes = 0.37–0.60), and a minor amount of bicadinanes (bicadinanes/$C_{30}$ hopane = 0.1–0.3) (Xiang and Ji, 2004; Huang et al., 2007), which indicates that it was derived from the Wenchang mudstone (Huang et al., 2003). According to the investigation made by Huang et al. (2006, 2007), the W10-3 trap formed during the early Miocene (21–18.5 Ma) and the Zhu III fault intersects throughout strata from the Wenchang Formation to the Zhujiang Formation. It may have trapped the later-generated oil from the Wenchang mudstone. The oil of the W15-1 petroleum pool, located at the Shenhu Uplift (Fig. 2), was also sourced mainly from the Wenchang mudstone based on a recent investigation made by Huang et al. (2006). The 2D basin modeling result from the present study also indicates that the petroleum can migrate toward the Shenhu Uplift to reach the W15-1 structure (Fig. 12).

## 4. Summary

We have developed an approach to identify deeply-buried source rocks. Through a case study of the W9-2 petroleum pool in the Pearl River Mouth Basin, South China Sea, the following results have been attained.

(1) The fluid inclusions in the reservoir sandstone of the W9-2 petroleum pool have recorded its oil-charging time from about 18 Ma to 3.5 Ma, and its gas-charging time from 4.5 Ma to the present. The kinetic modeling indicates that the main stages of oil generation of the Wenchang mudstone and the Enping mudstone occurred during 28–20 Ma and 20–12 Ma, respectively, and that the gas generated from the Enping mudstone has a similar $\delta^{13}C_1$ value with the reservoir gas.
(2) Results from a 2D basin modeling indicate that the well-developed syn-sedimentary faults in the central area of the Wenchang A sag may have connected the Enping Formation to the overlaying reservoir rock to provide a pathway for

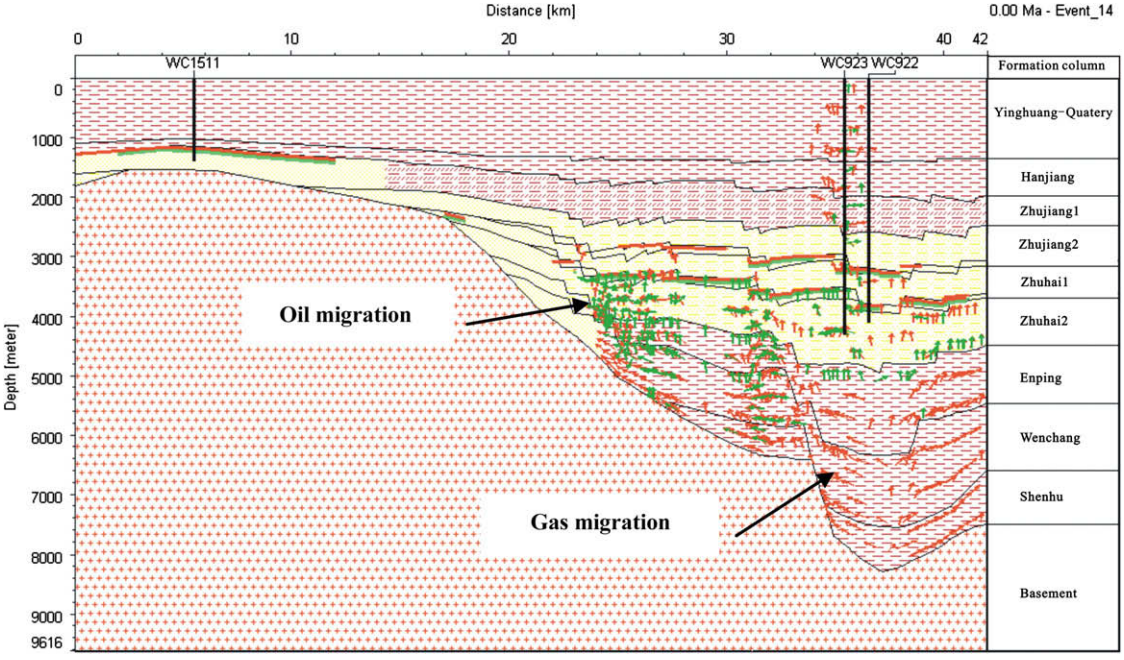


**Fig. 12.** A 2D modeling result at present day along a section across the southern part of the Wenchang A sag, showing the migration directions and possible reservoirs of the petroleum from the Wenchang and Enping formations. See details in text.

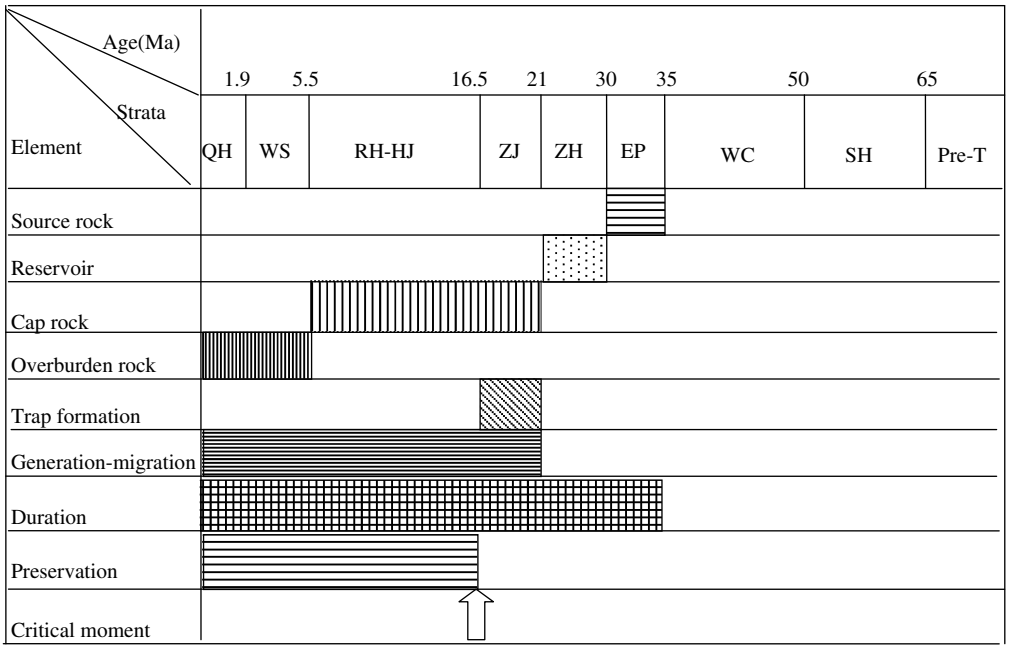


**Fig. 13.** Event chart of the petroleum system from the central area of the Wenchang A sag. QH: Qionghai Formation; WS: Wanshan Formation; RH: Yuehai Formation; HJ: Hanjiang Formation; ZJ: Zhujiang Formation; ZH: Zhuhai Formation; EP: Enping Formation; WC: Wenchang Formation; SH: Shenhu Formation; Pre-T: Pre-Tertiary.

petroleum migration into the reservoir. The petroleum generated from the Wenchang Formation may have migrated laterally toward the marginal faults of the sag and then migrated upward to shallow strata.

(3) We propose a new petroleum system in the central area of the Wenchang A sag. The Enping mudstone serves as the main source rock, the Zhuhai Formation as the reservoir and their overlaying strata as the sealing rock. The exploration in this area should focus on the petroleum sourced from the Enping mudstone. The petroleum generated from the Wenchang mudstone has contributed to the earlier-formed traps along the deep marginal faults of the sag and the trapping structures in the uplifted areas around the sag.

## Acknowledgements

The authors are indebted to Dr. Andrew Hanson and two anonymous reviewers for their insightful comments and suggestions that have significantly improved the manuscript. This work was financially supported by the Natural Science Fund for Distinguished Young Scholars (Grant No. 40625011), the Key Project of Chinese Academy of Science (Grant No. KZCX2-YW-114) and the Earmarked Fund of the State Key Laboratory of Organic Geochemistry (Grant No. SKLOG2008A01). This is contribution No.IS1050 from GIGCAS.

## References

Aplin, A.C., Larter, S.C., Bigge, M.A., Macleod, G., Swarbrick, R.E., Grunberger, D., 2000. PVTX history of the North Sea's Judy oilfield. Journal of Geochemical Exploration 69-70, 641–644.

Aplin, A.C., Macleod, G., Larter, S.R., Pedersen, K.S., Sorensen, H., Booth, T., 1999. Combined use of confocal laser scanning microscopy and PVT simulation for estimating the composition and physical properties of petroleum in fluid inclusions. Marine and Petroleum Geology 16, 97–110.

Editional Committee of Petroleum Geology of China (ECPGC), 1992. Petroleum Geology of China (No. 6). Petroleum Industrial Press, Beijing, 682 pp. (in Chinese).

Feng, Z.Q., Liu, C.L., 1999. Geological characteristics of reservoir and caprock in Wenchang A sag of the Pearl River Mouth Basin. China Offshore Oil and Gas 13 (6), 421–428 (in Chinese).

Gan, H.J., 2006. Accumulation History and Formation Mechanism of Petroleum Pools in Wenchang A Sag, Western Pearl River Mouth Basin. Ph.D thesis. Guangzhou Institute of Geochemistry, Chinese Academy of Sciences, 132 pp. (in Chinese).

Gao, X.L., Xiao, X.M., Zhao, B.Q., 2004. Petroleum generation history of early Tertiary source rocks in the Bozhong Depression of the Bohai Bay Basin. Acta Sedimentogica Sinica 22 (2), 359–364 (in Chinese).

GeolsoChem Corporation, 2003. GOR-Isotope. Version 1.48.

George, S.C., Krieger, F.W., Eadington, P.J., Quezada, R.A., Greenwood, P.F., Eisenberg, L.I., Hamilton, P.J., Wilson, M.A., 1997. Geochemical comparison of oil-bearing fluid inclusions and produced oil from the Toro Sandstone, Papua New Guinea. Organic Geochemistry 26, 155–173.

Gong, Z.S., 2004. Tectonic movement and petroleum pool formation in offshore area of China. Geoscience 29, 513–517 (in Chinese).

Hamilton, P.J., Kelly, S., Fallick, A.E., 1989. K–Ar dating of illite in hydrocarbon reservoirs. Clay Minerals 24, 215–231.

Hao, F., Zou, H.Y., Gong, Z.Y., Deng, Y.H., 2007. Petroleum migration and accumulation in the Bozhong sub-basin, Bohai Bay basin, China: significance of preferential petroleum migration pathways (PPMP) for the formation of large oilfields in lacustrine fault basins. Marine and Petroleum Geology 24, 1–13.

Hosgormez, H., Yalcin, M.N., 2005. Gas-source rock correlation in Thrace Basin, Turkey. Marine and Petroleum Geology 22, 901–916.

Huang, B.J., Xiao, X.M., 2002. Multiphase natural gas migration and accumulation and its relation to diapir structure in the DF1-1 gas field, South China Sea. Marine and Petroleum Geology 19 (7), 861–872.

Huang, B.J., Xiao, X.M., Zhang, M.Q., 2003. Geochemistry, grouping and origins of crude oils in the Western Pearl River Mouth Basin, offshore South China Sea. Organic Geochemistry 34, 993–1008.

Huang, B.J., Xiao, X.M., Liu, D.H., 2006. Geological and Geochemical Conditions of Petroleum and Accumulation in the Wenchang A Sag, Pearl River Month Basin, South China Sea. An internal report from a contract project between the CNOOC Ltd and Guanzhou Institute of Geochemistry. Chinese Academy of Sciences, 235 pp. (in Chinese).

Huang, B.J., Li, Z.L., Li, L., 2007. Formation characteristics and distribution of petroleum pools in the Wenchang Depression. China Offshore Oil and Gas 19 (6), 361–367 (in Chinese).

James, A.T., 1983. Correlation of natural gas by use of carbon isotopic distribution between hydrocarbon components. AAPG Bulletin 67 (7), 1176–1191.

Ji, H.Q., Wang, X.H., 2004. The potential of oil and gas exploration in Wenchang A sag of the Pearl River Mouth Basin. Natural Gas Geosciences 15 (3), 238–242 (in Chinese).

Jiang, Z.S., Lao, X., Li, Z.S., 2000. Carbon isotope compositions of benzene and toluene as a new parameter in gas-source correction. Geochemistry 29 (4), 410–415 (in Chinese).

Justwan, H., Meisingset, I., Dahl, B., Isaksen, G.H., 2006. Geothermal history and petroleum generation in the Norwegian South Viking Graben revealed by pseudo-3D basin modeling. Marine and Petroleum Geology 23 (8), 791–819.

Lampe, C., Kornpihl, K., Sciamanna, S., Zapata, T., Zamora, G., Varadé, R., 2006. Petroleum systems modeling in tectonically complex areas – a 2D migration study from the Neuquen Basin, Argentina. Journal of Geochemical Exploration 89 (1–3), 201–204.

Lao, X., Hu, G.Y., Zhang, F.D., 2002. Gas-source correction for Qingmichu Ordovician hidden reservoir. Petroleum Exploration and Development 29 (4), 41–43 (in Chinese).

Li, J., Hu, G.Y., Xie, Z.Y., 2001. Formation of Large and Middle Scale Natural Gas Pools by Physical and Chemical Modeling. Petroleum Industrial Press, Beijing, 100 pp. (in Chinese).

Liang, X.Q., 1989. Petroleum formation conditions of the Wenchang A sag. China Offshore Oil and Gas 3 (6), 27–35 (in Chinese).

Liang, D.G., Chen, J.P., 2005. Problems on oil-source correction in high and over mature areas of China petroleum-bearing marine basins. Petroleum Exploration and Development 32 (4), 8–15 (in Chinese).

Liewig, N., Clauer, N., Sommer, F., 1987. Rb–Sr and K–Ar dating of clay diagenesis in Jurassic sandstone oil reservoir, North Sea. AAPG Bulletin (12), 1467–1474.

Lin, X., Sun, Z., 1999. The conditions of natural gas pool forming in Wenchang A sag. Natural Gas Industry 19 (1), 47–51 (in Chinese).

Liu, B., Shen, K., 1999. Thermodynamics of Fluid Inclusions. Geological Publishing House, Beijing, pp. 23–68 (in Chinese).

Liu, G.Q., Jiang, C.G., Pan, W.L., 2003a. Light hydrocarbon analysis from dry gas and its application in gas-source correction: a case study of the Jurassic reservoir in the southeastern area of the Sichuan Basin. Petroleum Experimental Geology 25, 585–589 (in Chinese).

Liu, J.P., Geng, A.S., Xiong, Y.Q., Li, Y.X., Zhu, G.J., Zhang, Y.X., Li, Y.S., 2007. Application of carbon and hydrogen isotope ratios of normal alkanes in oil-source correction. Xinjiang Petroleum Geology 28 (1), 104–108 (in Chinese).

Liu, W.H., Sun, M.L., Xu, Y.C., 2001. Rare gas isotope of natural gas and its application to gas source tracing in the Ordos Basin. Chinese Science Bulletin 46 (22), 1902–1905 (in Chinese).

Liu, D.H., Xiao, X.M., Mi, J.K., Li, X.Q., Shen, J.K., Song, Z.G., Peng, P.A., 2003b. Determination of trapping pressure and temperature of petroleum inclusions using PVT simulation software – a case study of Lower Ordovician carbonates from the Lunnan Low Uplift, Tarim Basin. Marine and Petroleum Geology 20, 29–43.

Littke, R., Cramer, B., Gerling, P., 1999. Gas generation and accumulation in the West Siberian Basin. AAPG Bulletin 83, 1642–1665.

Lutz, R., Littke, R., Gerling, P., Bönnemann, C., 2004. 2D numerical modeling of hydrocarbon generation in subducted sediments at the active continental margin of Costa Rica. Geology, Marine and Petroleum Geology 21 (6), 753–766.

Magoon, L.B., Dow, W.G., 1994. The Petroleum System from Source to Trap, vol. 60. AAPG Memoir, ISBN 0-89181-338-1.

Mann, U., Hantschel, T., Schaefer, R.G., 1997. Petroleum migration: mechanisms, pathways, efficiencies and numerical simulations. In: Welte, D.H. (Ed.), Petroleum and Basin Evolution. Springer, pp. 468–490.

Mi, J.Q., Xiao, X.M., Liu, D.H., 2004. Determination of paleo-pressure for a natural gas pool formation based on PVT characteristics of fluid inclusions in reservoir rocks. Science in China (Ser. D) 47 (6), 507–513.

Mclimans, R.K., 1987. The application of inclusion to migration of oil and diagenesis in petroleum reservoirs. Applied Geochemistry 2, 585–603.

Munz, I.A., 2001. Petroleum inclusions in sedimentary basins: systematics, analytical methods and applications. Lithos 55, 193–210.

Parnell, J., Middleton, D., Honghan, C., Hall, D., 2001. The use of integrated fluid inclusion studies in constraining oil charge history and reservoir compartmentation: example from the Jeanned Arc Basin, offshore Newfoundland. Marine and Petroleum Geology 18, 535–549.

Pepper, A.S., Corvit, P.J., 1995. Simple kinetic models of petroleum formation. Marine and Petroleum Geology 12 (30), 291–319.

Peters, K.E., Moldowan, J.M., 1993. The Biomarker Guide: Interpreting Molecular Fossils in Petroleum and Ancient Sediments. Prentice Hall Inc, 260 pp.

Robinson, B.W., Himer, A.V., 1991. Stable carbon and sulfur isotope distributions of crude oil and source rock constituents from Burgan and Raudhatain oil field (Kuwait). Chemical Geology 86, 295–306.

Inan, S., Yalqm, M.N., Guliev, I.S., Kuliev, K., Feizullayev, A.A., 1997. Deep petroleum occurrences in the Lower Kura Depression, South Caspian Basin, Azerbaijan: an organic geochemical and basin modeling study. Marine and Petroleum Geology 14, 73l–762.

Schneifer, F., Wolf, S., 2000. Quantitative HC potential evaluation using 3D basin modelling: application to Franklin structure, Central Graben, North Sea, UK. Marine and Petroleum Geology 17, 841–856.

Schoell, M., 1980. The hydrogen and carbon isotopic compositions of methane from natural gases of various origins. Geochimica et Cosmochimica Acta 44, 649–662.

Seifert, W.K., Moldowan, J.M., 1978. Applications of steranes, terpanes, and monoaromatics to the maturation, migration and source of crude oils. Geochimica et Cosmochimica Acta 42, 77–95.

Stahl, W.J., 1978. Source rock-crude oil correlation by isotopes type-curves. Geochimica et Cosmochimica Acta 42 (10), 1573–1577.

Sun, Y.G., Sheng, G.Y., Peng, P.A., 2000. Compound specific isotope analysis as a tool for characterizing coal-sourced oils and interbedded shale sourced oils in coal measure: an example for Turpan Basin, Northwestern China. Organic Geochemistry 31, 1349–1362.

Swarbricka, R.E., Osbornea, M.J., Grunbergera, D., Yardleyb, G.S., Macleodc, G., Aplin, A.C., Larterc, S.R., Knightf, I., Auldf, H.A., 2000. Integrated study of the Judy Field (Block 30/7a) — an over-pressured Central North Sea oil/gas field. Marine and Petroleum Geology 17, 993–1010.

Tang, Y., Perry, J.K., Jenden, P.D., Schoell, M., 2000. Mathematical modeling of stable carbon isotope ratios in natural gases. Geochimica et Cosmochimica Acta 64, 2673–2687.

Tao, S.Z., Zhang, B.M., Zhao, C.Y., 2003. Application of fluid inclusion analysis in tracing petroleum sources – a case study of the Sichuan Basin. Lithology 19 (2), 327–336 (in Chinese).

Tian, H., Xiao, X.M., Wilkins, R.W.T., 2007. Gas source of the YN2 gas pool in the Tarim Basin-evidence from gas generation and methane carbon isotope fractionation kinetics of source rocks and crude oils. Marine and Petroleum Geology 24, 29–41.

Tissot, B.P., Welte, D.H., 1984. Petroleum Formation and Occurrence. Springer-Verlag, New York, Berlin, Heidelberg, 456 pp.

Tissot, B.P., Pelet, R., Ungerer, P., 1987. Thermal history of sedimentary basins: maturation indices and kinetics of oil and gas generation. AAPG Bulletin 71, 1445–1466.

Ungger, P., Pelet, R., 1987. Extrapolation of the kinetics of oil and gas formation from laboratory experiments to sedimentary basins. Nature 327, 52–54.

Ungerer, J., Burrus, B., Doligez, P.Y., Bessis, F., 1990. Basin evaluation by integrated two-dimensional modeling of heat transfer, fluid flow, hydrocarbon generation, and migration. AAPG Bulletin 74 (3), 309–335.

Wang, F., Zeng, Q.H., Liu, D.H., Xiao, X.M., Shen, J.G., Gan, H.J., 2006. Formation conditions of petroleum inclusion in diabase and petroleum pool formation in the Linyi Depression. Geochemistry 35 (3), 285–294 (in Chinese).

Wang, J.B., Xiao, X.M., Gao, R.T., 2002. Dating petroleum events by means of bitumen reflectance in the lower Ordovician strata of the Lunnan Low Uplift, Tarim Basin. Chinese Sedimentary Acta 20 (2), 320–325 (in Chinese).

Wang, L.Z., Mo, D.T., Peng, P.A., 2005. Ar–Ar dating of diagenetic illites and its application in timing gas emplacement in gas reservoirs. Earth Science – Journal of China University of Geosciences 30 (1), 78–83.

Xiang, L., Ji, H., 2004. Natural Gas Appraisal and Proposal of Drilling Wells in the Wenchang 10-3 Structural Zone of Wenchang A Sag, Western Pearl River Mouth Basin. CNOOC Limited, Zhanjiang. Internal report (in Chinese).

Xiao, X.M., Liu, D.H., Fu, J.M., 1996. Multiple phases of hydrocarbon generation and migration of Tazhong petroleum system. Organic Geochemistry 25 (3/4), 191–197.

Xiao, X.M., Song, Z.G., Liu, D.H., Liu, Z.F., Fu, J.M., 2000. The Tazhong hybrid petroleum system, Tarim Basin, China. Marine and Petroleum Geology 17, 1–12.

Xiao, X.M., Liu, D.H., Fu, J.M., 2001. Dating hydrocarbon generation and migration based on bitumen reflectance. Chinese Science Bulletin 46 (7), 611–616.

Xiao, X., Liu, Z., Mi, J., Liu, D., Shen, J., Song, Z., 2002. Dating formation of natural gas pools using fluid inclusion data from reservoirs. Chinese Science Bulletin 47, 1567–1572.

Xiao, X.M., Zeng, Q.H., Tian, H., Wilkins, R.W.T., Tang, Y.C., 2005. Origin and accumulation model of the AK-1 natural gas pool from the Tarim Basin, China. Organic Geochemistry 38, 1285–1298.

Xiao, X.M., Min, X., Tian, H., Wilkins, R.W.T., Huang, B.J., Tang, Y.C., 2006. Determination of source area of the Ya13-1 gas pool in the Qiongdongnan Basin, South China Sea. Organic Geochemistry 37, 990–1002.

Zhang, S.C., Moldowan, J.M., Li, M.W., 2001. An abnormal distribution of biomarkers in pre-Cambrian strata and its biological significance. Science in China (D) 31 (4), 34–37 (in Chinese).

Zhang, S.C., Liang, D.G., Gong, Z.S., Wu, K.Q., Li, M.W., Song, F.Q., Song, Z.G., Zhang, D.J., Wang, P.R., 2003. Geochemistry of petroleum systems in the eastern Pearl River Mouth Basin: evidence for mixed oils. Organic Geochemistry 34, 971–991.

Zhang, C.M., Li, S.T., Yang, J.M., Yang, S.K., Wang, J.R., 2004. Petroleum migration and mixing in the Pearl River Mouth Basin, South China Sea. Marine and Petroleum Geology 21, 215–224.